Vol. 44, No. 1 (2022) 87-96, DOI: 10.24874/ti.1074.03.21.07

Tribology in Industry

www.tribology.rs

RESEARCH

Evaluation of the Hardness and Wear Resistance of Alloyed Coatings From Fastening CuSn/CrxCy Mixture Hardened by Plasma and Laser

Van Trieu Nguyen[a], Natalya Anatolyevna Astafeva[a], Aleksandr Gennadievich Tikhonov[a], Andrey Evgenievich Balanovskiy[a,*], Van Huy Vu[a]

[a]*National Research Irkutsk State Technical University, Russia.*

Keywords:

Cu-Sn
CrxCy
Plasma treatment
Laser treatment
Reflow
Cracks
Microhardness
Wear resistance

* Corresponding author:

Andrey Evgenievich Balanovskiy
E-mail: fuco.64@mail.ru

Received: 15 March 2021
Revised: 31 May 2021
Accepted: 16 July 2021

A B S T R A C T

This article provides an assessment of the possibility of increasing the wear resistance of the alloyed surface layer for steel St3 during plasma and laser heating of the applied surface pre-coating of the mixture of CuSn/CrxCy alloys. Plasma is more suitable for reflow a pre-deposited layer of CuSn/CrxCy with a wide range of particle sizes than laser treatment. As a result, plasma coatings have a high hardness (460-700 HV) compared to laser coatings (250-500 HV). The tests carried out showed that the wear resistance increases in the following order: Steel St3 <laser coating (CuSn +% 20 OK 84.78) <plasma coating CuSn <plasma coating CuSn +% 20 OK 84.78. The results obtained showed that plasma heating of a mixture of bronze and chromium carbide possibly provides the development of technologies for surface hardening of carbon steel.

1. INTRODUCTION

The increased hardness and wear resistance of the surface is the main factor in ensuring the resistance of the material surface to mechanical stress, such as wear, impacts, cracking, and others. To form alloyed coatings on machine parts and tools, surface heating methods are used by highly concentrated heat sources: plasma arc [1,2], plasma laminar jet [3,4], laser [5, 6]. The essence of these methods is that the melting of the investigated powder alloy occurs at high temperatures and heat transfer under the influence of highly concentrated energy flows [1-7]. Surface alloying with laser heating makes it possible to obtain layers with a thickness of up to 300 microns under pulsed exposure, and up to 700-800 microns with continuous radiation. With plasma heating, it is possible to obtain an alloyed layer up to 1–2 mm deep [5,6]. Copper-tin (CuSn) alloys are commonly used as plain bearing materials due to their high thermal conductivity,

electrical conductivity, self-lubrication, excellent wear resistance and corrosion resistance [8,9]. Copper is often present in many alloys, the most common of which is bronze. The use of copper alloys to create a protective coating is available in various processing methods, such as sputtering (cold and thermal), laser processing, and others [10-13]. However, studies of mixtures of copper, chromium, and iron using these methods have not yet fully yielded the expected results, since differences in the properties of immiscible phases still make it difficult to create coatings with a low degree of defects and high hardness. It is known that Cu-Sn alloy coatings have low hardness [14,15], therefore, at present, many studies are directed towards the tendency of adding a hardening component to the original composition. Regardless of the various methods, there are strengthening additives, such as examples of WC, Al_4C_3, Al_2O_3 [16]. Elements such as Ni, Fe, Co, Cr are added to CuSn alloys, respectively, to improve their microstructure and properties. Carbides of metals such as chromium are widely used. An increase in the hardness of a coating based on a tin-bronze alloy during plasma arc treatment using an addition of an iron-based alloy containing chromium carbides was demonstrated in [8-9], but the maximum hardness did not exceed 400 HV.

It is well known [2-6] that for any type of coating the following features must be achieved: absence of defects (cracks, pores), high uniformity, hardness and sufficient adhesion force between the coating and the main substrate. To eliminate the disadvantages of coatings (pores, low adhesive force, heterogeneity) in thermal spraying technology, some authors used methods of remelting thermal sprayed coatings with a thin surface layer of metal. In other works, the surfacing of metals using laser and plasma heat sources gives good results in terms of hardness, while simultaneously increasing the resistance to corrosion [6-10]. Expanding research into the use of various energy sources such as plasma arc, laser and various additives to create coatings provides additional opportunities to minimize operating costs while maintaining preferred quality. Our review of the literature shows that so far there are few experimental works on the effect of adding Cr particles and their mass fraction on the microstructure of a bronze alloy, and there are practically no works on surface modification in the open press.

The purpose of this work is to evaluate the hardness values of surface coatings during plasma and laser heating of mixtures of Cu-Sn alloy and Weartrode 60 T (OK 84.78)(ESAB) electrode coating. The article presents the results of studies of microstructures and distribution of hardness over the cross section of the obtained coatings.

2. EXPERIMENT

As a surface coating, we used a mixture of powder alloys PRV-BrO10 CuSn (manufactured by JSC Polema) and a coating of the welding electrode OK 84.78 (ESAB). Welding surfacing electrodes OK 84.78 (ESAB) by composition contain: 4.5% C, 1.2% Mn 1.2% Si, 33% Cr. For preparing the powder pre-coating from the OK 84.78 electrode coating, pliers were used to remove the coating, then it was rolled between two rolls until grinding - this is the first fraction. Then they took a part of the first fraction and additionally ground it in a porcelain cup using a pestle - the second fraction was obtained. The particle size distribution of the studied powder alloys was determined by the ANALYSETTE 22 laser analyzer and is shown in Table 1. The resulting powders were mixed with a binder (using stationery glue Erich Krause) to form a paste, which was then manually applied to the samples and dried at a temperature of 373 K. On all samples, the pre-coating was applied at a fixed thickness of 0.25 mm. Steel samples were rectangular plates with dimensions 70×25×10 mm. The surface of the samples was ground to a roughness Ra=0.2 μm. An installation described in detail in [7] was used as a source of plasma heating. Plasma heating mode: current strength 140 A; the speed of movement of the samples is 2.7 mm/s; gas (argon) feed rate 10 l/min, the gap between the coating layer and the electrode is 4-5 mm. After cutting, polishing and etching the obtained samples, their microstructures were studied using a MET-2 metallographic microscope, and the hardness of the coatings was measured using an HMV-G21 hardness tester under a load of 0.2 kg. The selected compositions of mixtures and cooling modes are given in Table 2. In the course of operation, a pulsed lamp-pumped Kvant 15 laser power supply was used, its characteristics are presented in Table 3.

Table 1. Particle size distribution of PRV-BrO10 alloys and OK 84.78 coatings by percentage.

Fraction of particles,%	Particle diameter, μm		
	PRV-BrO10	First fraction OK 84.78	Second fraction OK 84.78
5	11.94	0.98	1.66
10	27.79	1.74	3.67
20	39.52	4.62	10.93
30	47.74	13.31	18.87
40	55.16	22.93	28.40
50	62.53	36.42	43.42
60	70.45	74.74	76.26
70	79.46	124.31	126.79
80	90.48	171.30	164.17
90	106.79	223.57	207.44
95	120.65	262.01	239.95
98	135.91	303.76	275.74
99	146.64	329.54	297.83

Table 2. Compositions of mixtures of alloys and modes of cooling of coatings.

№ Sam.	Fraction OK 84.78	The composition of the mixture	Mode of cooling
1	-	CuSn	water
2	First	CuSn + 10% OK 84.78	water
3	First	CuSn + 20% OK 84.78	water
4	Second	CuSn + 10% OK 84.78	water
5	Second	CuSn + 20% OK 84.78	water
6	Second	CuSn + 10% OK 84.78	air
7	Second	CuSn + 20% OK 84.78	air
8	Second	CuSn + 30% OK 84.78	air

Table 3. Parameters of Laser source Kvant 15.

Parameter name	Value
Number of pump lamps	one or two
Pulse repetition rate	1 - 20 Hz, single
Drive voltage	750 V
Drive voltage discreteness	1 V
Pump current pulse duration	0.1-6.0 ms
Discreteness of the change in the duration of the pump current	0.1 ms
Working hours	partial discharge
Charging module power	5 kW
Standby current	0.6 A
Communication interface	RS232 *
Information display	LCD display
External sync input	5 V, 10 μs *
Sync output	5 V, 10 μs *
Attenuator control output	2 * 27V
Output sync delay	0-6 ms *

Figure 1 shows the process of laser surface alloying of samples with applied coating.

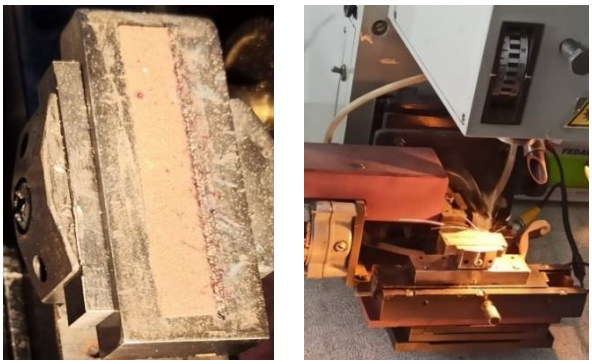

(a) (b)

Fig. 1. Process of laser surface alloying: (a) sample with applied coating; (b) laser alloying of the sample in action.

For wear testing, a sample preparation is given. After plasma heating and cooling, the sample was cut to get them in the form of a parallelepiped with dimensions of 12x5x10 mm. Such a sample has already been used in the work of Huy [17]. In this case, the working surface was in contact with the abrasive, and the other was filled with acrylic resin in the form of a cylinder for subsequent fixation on the holder of the Struers Tegramin-25 grinding and polishing machine. The fixed abrasive wear test was carried out on a grinding and polishing machine. Wear resistance was determined for samples of coatings before and after plasma hardening, by rotary movements on the surface of grinding paper based on silicon carbide. During the tests, the pressing force of the samples was regulated with a force from 5 N to 50 N, the samples exposed to a certain load were pressed against a rotating aluminum disk and fixed on it with an abrasive cloth. When the aluminum disk rotates, the holder with the sample moves from the periphery to the center and back. The wear resistance index of coatings, equal to the ratio of changes in the mass of the standard and the sample. Samples of steel St3 without plasma hardening were taken as a standard. The abrasive materials used for testing are silicon carbide (SiC) with particle sizes from 63 to 80 μm in accordance with GOST 3467-80 [18].

3. RESULTS AND DISCUSSION

After plasma and laser heating of coated samples, subsequent cooling and cutting, the appearance and cross-section of a typical surface layer are shown in Figure 2. To evaluate

the coating, its central part was cut out, where the processing mode was stable. In cross-section, the surface layer of a typical sample (Fig. 2) consists of an alloyed layer (A), a fused layer (B), and a heat-affected zone (C). The dilution factor of the base metal is calculated in the formula (1):

$$K = B / (A + B) \quad (1)$$

Where A, B are the areas of the clad layer of the coating and the molten metal of the substrate, respectively (shown in Fig. 2b).

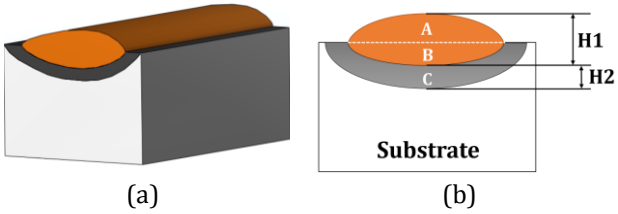

Fig. 2. Typical appearance (a) and cross-section of the coating (b) after plasma treatment.

Corresponding to the sample number in Table 2, the cross section of the plasma-coated samples is shown in Table 4. In the case of CuSn alloy only, the coating is formed with cracks, has a high depth and a high dilution ratio of the substrate. This is due to the soft alloy particles, which are more conducive to heat transfer from the source to the substrate. It can be seen that coatings with finer particles (second fraction) and compositions of 10% OK 84.78 under № 4, 6 have a greater depth of fusion, about 1300 μm (H1). In contrast, coatings with coarser particles (№ 2, 3) have a shallower reflow depth (about 900 microns). The depth of the heat-affected zone (HAZ) shown in Table 4 (H2) from the boundary of the coating fusion zone has differences between the types of coatings used depending on the fineness of the alloy powder particles. With coarser particles, coating samples № 2, 3 have values of the H2 index in the range of 1800-1900 μm. The thickness of the doped H1 layer is 800-900 μm. When using the composition of the mixture with more dispersed particles of the coating № 4, 5, the H1 index is more than 1000 μm, the H2 values are 2000-3000 μm. This is due to the faster melting of the highly particulate coating and heat transfer. Coating of sample № 8 has multiple cracks and pores.

Table 4. Cross-section of coatings and their characteristics.

Cross-section	H1, μm	H2, μm	K, %
 № 1	1235	1650	75
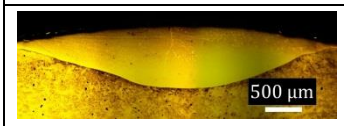 № 2	900	1800	57
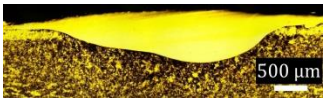 № 3	850	1900	54
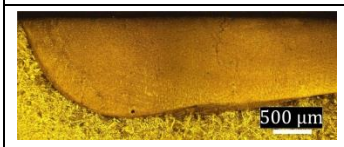 № 4	1300	3000	69
 № 5	1060	2050	55
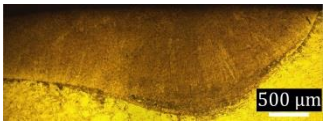 № 6	1360	2900	74
 № 7	1090	2300	51
 № 8	960	1500	47

In addition, increasing the chromium carbide content prevents the alloy mixture from fusing to the substrate due to the difference in melting temperature and particle size. Therefore, in a coating with a lower chromium carbide content (10% OK 84.78), the substrate dilution coefficient (K) is higher than in other 20% OK 84.78. It should be noted that after plasma heating, the samples were immediately additionally cooled with water/air, and the surface temperature was measured using a pyrometer. It was found that immediately after plasma heating and

melting of the coating within 1-2 seconds, the temperature drops sharply to 500-600 °C, and after 1-2 minutes it reaches 300-350 °C. It is noted that the cooling mode does not significantly affect the depth of the HAZ, but strongly affects the hardness of the coatings.

In figures 3, 4 has showed the distribution of the hardness of the cross-section of the surface layer after melting of the pre-coatings from the CuSn/CrxCy mixture along the depth of the surface layer. The hardness of the alloyed layer has increased.

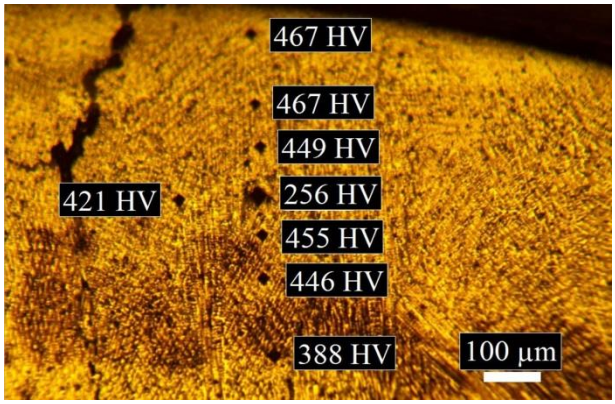

(a)

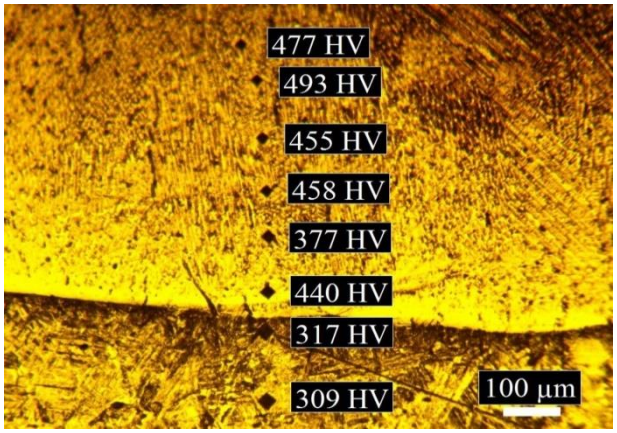

(b)

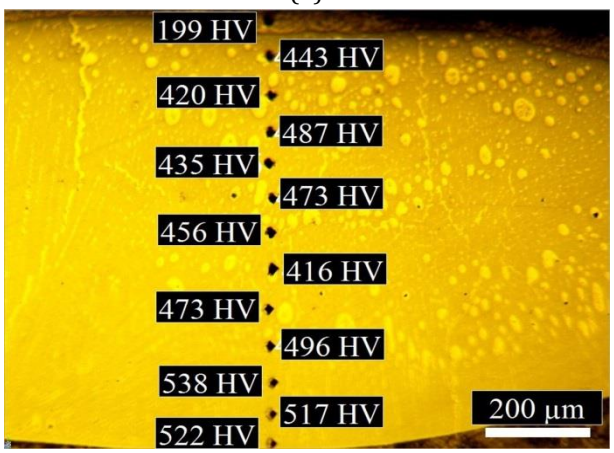

(c)

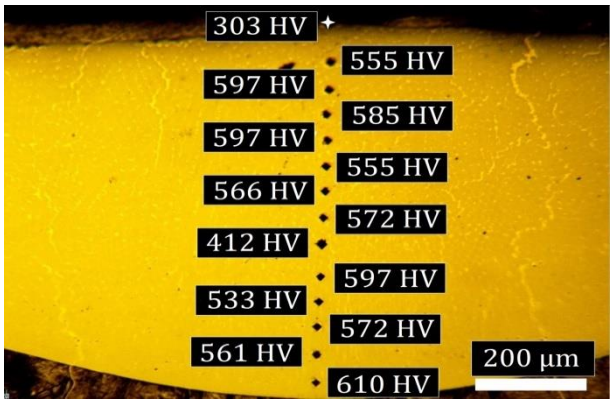

(d)

Fig. 3. Distribution of hardness along the depth of the alloyed layer after plasma treatment of the pre-coating of mixture CuSn + CrxCy: (a, b)-№1, (c)-№2, (d)-№3.

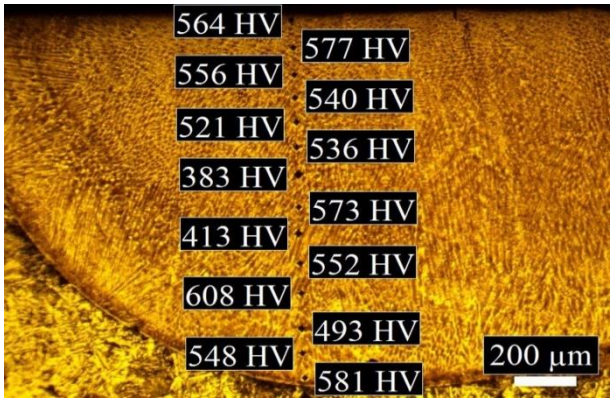

(a)

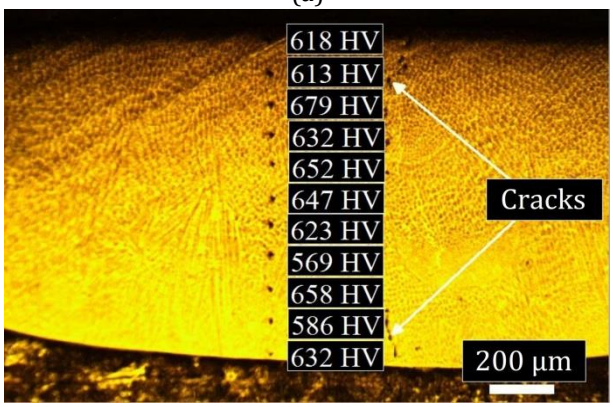

(b)

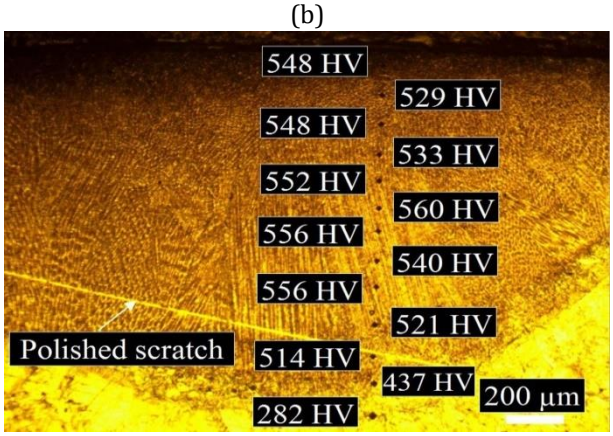

(c)

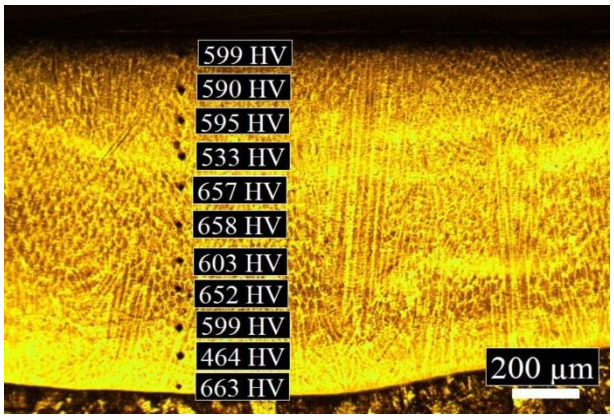

(d)

Fig. 4. Distribution of hardness along the depth of the alloyed layer after plasma treatment of the pre-coating of mixture CuSn/CrxCy: (a)-№4, (b)-№5, (c)-№6, (d)-№7.

It can be seen that in one plasma treatment mode, the surface layer of the metal with a coating fraction of coarser particles (the first fraction of OK 84.78), the resulting surface layers are not yet completely saturated with chromium and have upper sublayers with low hardness (199 HV, 303 HV), shown in fig. 3 c, d. In the case of using the second fraction of the coating of smaller particles, the resulting surface layers are already more saturated, providing high hardness. In fig. 4. (b) from the water cooling mode, coating № 5 (20% OK 84.78) has a crack. According to the binary Cu–Sn phase diagram, the sequence of transformations occurring upon heating can be described as follows. First, Sn melts, then liquid Sn wets the Cu particles. Then, upon continuous heating, Cu interacts with Sn-rich zones, which is supported by Cu diffusion and leads to the gradual formation of the ε-phase, δ-phase and γ-phase.

At the cooling stage, the eutectoid decomposition γ → α (Cu) + δ occurred below 520 °C. In the course of analyzing the results, we came to the conclusion that by combining the CuSn phase diagram and the Fe–Cr–C phase diagram for a CuSn/CrxCy-based coating, the doped layer consists of a solid solution and compounds. The solid solution in the coatings based on CuSn and Fe–Cr–C are α (Cu, Sn) and γ (Fe), respectively, and the compounds $Cu_{10}Sn_3$ and M_7C_3 (M = Fe, Cr). The Cu-rich matrix of the doped layer consists of α (Cu, Sn) and $Cu_{41}Sn_{11}$, and the Fe-rich spheroid consists of γ (Fe) and M_7C_3 type carbides (M = Fe, Cr) [8-11].

It was found that an increase in the content of chromium carbide in the coating increases the likelihood of defects such as cracks and pores in the coating, for example, sample № 8 (30% OK 84.78). The distribution of hardness in the depth of the surface layer is shown in the graphs (fig. 5).

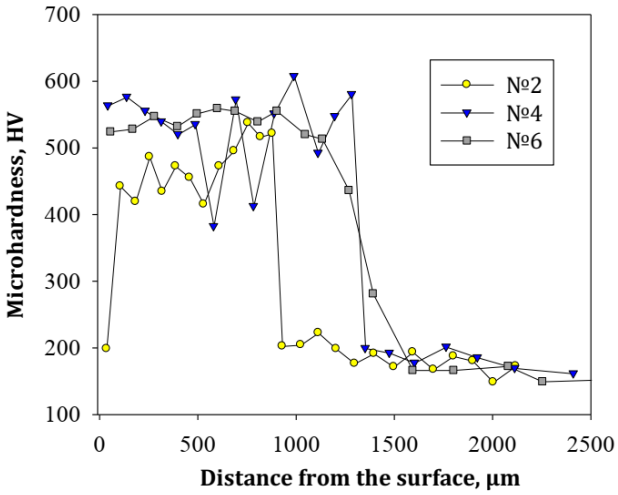

(a)

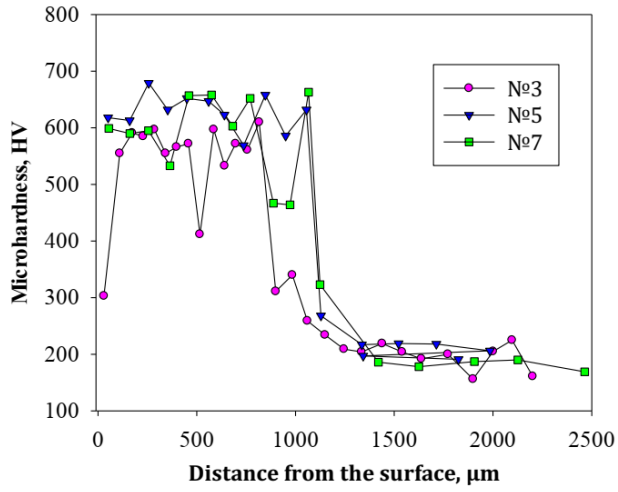

(b)

Fig. 5. Distribution of hardness of the cross-section of plasma coatings over depth: (a) CuSn + 10% OK 84.78; (b) CuSn + 20% OK 84.78.

It can be seen that coatings from the second fraction and with a higher content of chromium carbide give higher and uniform values of microhardness. The depth distribution of hardness values showed that coatings consisting of small particles have a greater depth. It was revealed that when the samples are cooled after plasma heating with water, the HAZ has a higher hardness than when cooled with air. It was found that the cooling of the coating with water after plasma heating leads to the concentration of the

hardness value in a thin surface layer of the metal. From graph 5 (a) it can be seen that some low hardness values of coating № 4 cooled with water can be associated with an uneven distribution of the strengthening component (low content of OK 84.78 - 10%). In the case of a higher content of OK 84.78, water-cooled coatings have more concentrated hardness values than air-cooled coatings (in Fig. 5 (b)). The measurement results show that the change in hardness also depends on the cooling mode. With a small degree of cooling ΔT, the number of nuclei is small. Under these conditions, a coarse grain of austenite will be obtained. With an increase in the degree of supercooling, the rate of formation of nuclei increases, their number increases, and the grain size in the solidified metal decreases.

Laser processing of samples with similar coating compositions was carried out with overlapping reflow tracks. Figure 6 shows the appearance of the laser-treated surface. Figures 7, 8 show the cross-section of the samples after laser treatment processing of alloys mixtures CuSn+10/20% OK 84.78. It can be seen that cracks appear in laser coatings on all reflow tracks with different zones. Many unmelted particles remain on the surface of the coating (fig. 6 (b)). The depth of reflow is 100 to 200 μm, which is much less than that of the samples after plasma reflow of the pre-coatings (fig. 7, 78). The heat affected zone also has a thin layer, below 50 microns. Due to the thin HAZ layer, cracks can reach down to the base metal.

In several reflow tracks, due to uneven mixing of the powder in the molten bath, we fix small depths of reflow of the surface layer of the metal. Obviously, when small areas of coating with narrow tracks of fusion (about 500 microns) of a laser beam are melted, the contribution of the content of each alloy in the mixture is not the same. In contrast, with a large plasma arc reflow tracks (5-6 mm), the coating melts more evenly.

(a)

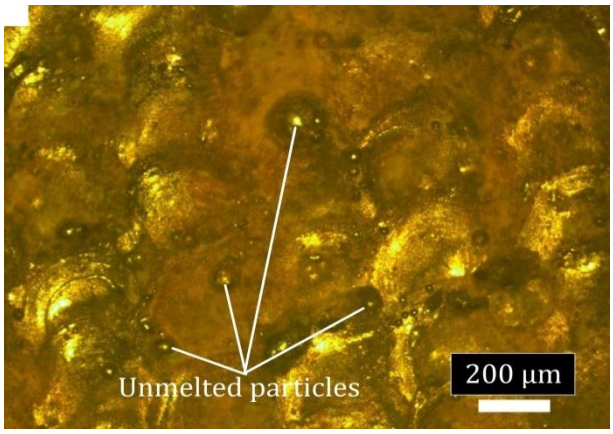

(b)

Fig. 6. Appearance of the laser-treated surface.

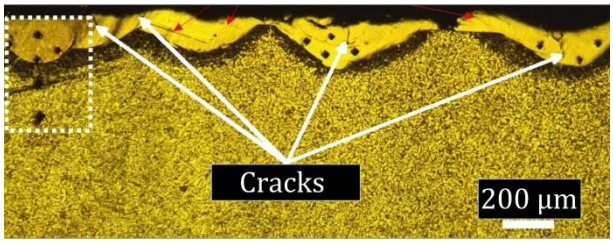

(a)

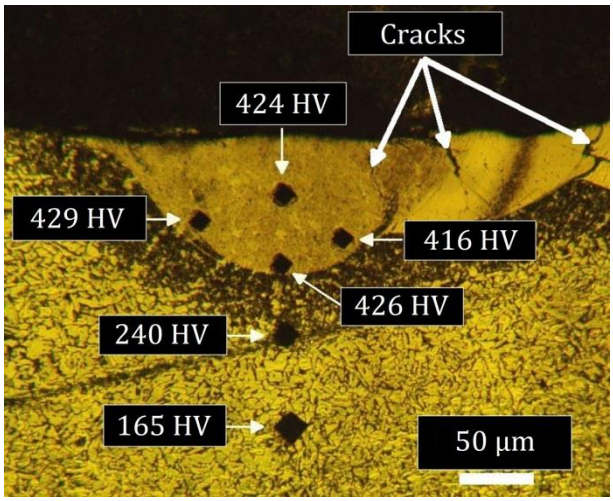

(b)

Fig. 7. Cross-sectional sections with measured microhardness values laser coating from mixture CuSn + 10% OK 84.78.

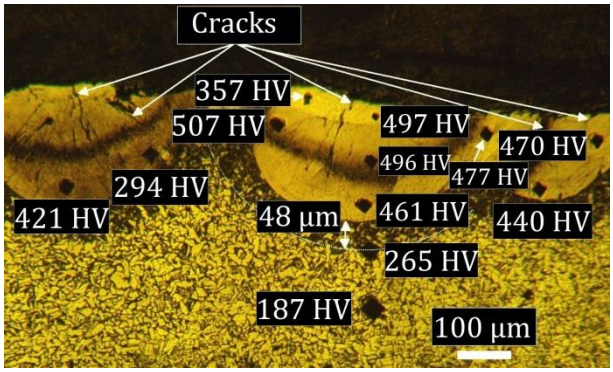

(a)

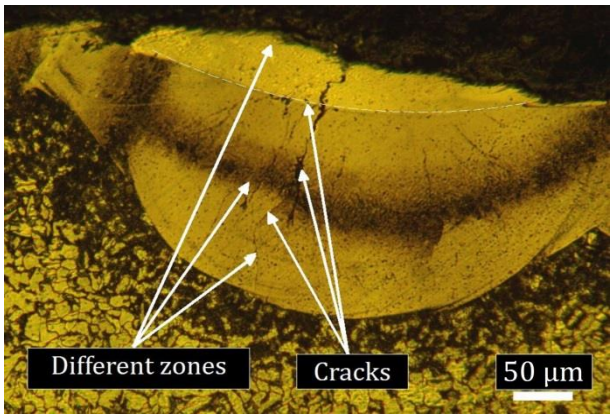

(b)

Fig. 8. Cross-sectional sections with measured microhardness values laser coating from mixture CuSn + 20% OK 84.78.

An alloy of the Cu-Sn system with a high Cu content is known to have most of the α-Cu phases, which do not have transformations in the form of carbide. It can be assumed that the short duration of laser heating is the reason for the incomplete saturation of the α-Cu phases in the coating; therefore, in combination with the uneven distribution of structural phases, the formation of cracks in the surface layer is caused.

The difference in depth between reflow baths and the appearance of microcracks indicate high demands on the technological parameters of laser processing, which are caused by many factors, including high uniformity of particle size and surface preparation. To compare the obtained coatings after plasma and laser treatment, statistical processing of the hardness values along the depth of the surface layer was carried out. The results of statistical processing are grouped using the graph "Box plot" in fig. 9.

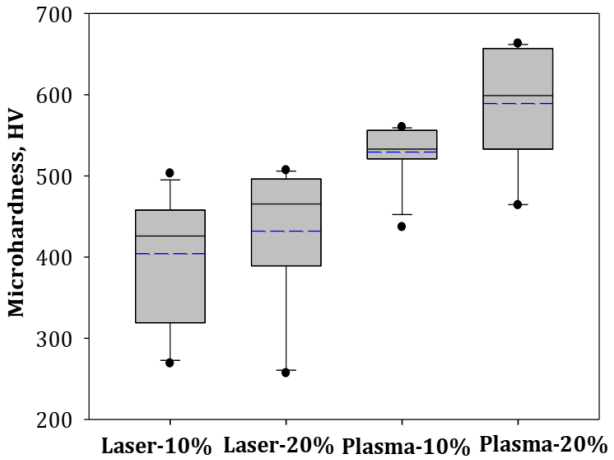

Fig. 9. Comparative dispersion of the microhardness of the cross section of laser and plasma coatings.

Comparative dispersion of microhardness values (fig. 9) is presented for the compositions of the CuSn + 10, 20% content of OK 84.78 with a more dispersed particle size. For coatings with a high chromium carbide content (20% OK 84.78), most of the microhardness values are higher than those with a lower chromium carbide content (10% OK 84.78).

Several values (median, quartile, minimum, maximum) in the dispersion show that 75% of the hardness values of the plasma coating with the addition of a mixture of 10% OK 84.78 and 100% of the values of the plasma coating hardness of 20% OK 84.78 are higher than for all values of the samples after laser processing. Plasma coating (20% OK 84.78) has the most concentrated distribution of hardness values. The studies carried out and the results obtained show the prospects for further work in increasing the strength and hardness of alloys of the Cu-Sn system. This is especially true for the formation of surface layers on various parts of machines and tools.

Of all the graphs shown in figure 10, all coatings are more wear resistant than the surface of St3 steel (uncoated). In the first case of 5 N load, the initial surface morphology of the laser coating had many defects, such as many microcracks between melt pots on an uneven surface. This leads to abrasion more quickly, i.e. very top subcoats peel off easily. Meanwhile, for CuSn coating, surface cracking may cause deterioration in wear resistance. In contrast, the CuSn coating with the addition of chromium carbide with a higher hardness, has a high wear resistance regardless of defects. As time increases, the curvature of the time-mass loss curve increases; indicates that the inner sublayers are significantly added with a reinforcing component with high uniformity, and also that the number of defects is reduced in them. This is also consistent with many studies related to the permeability and solubility of copper in iron and diffusion of chromium in steel [8-10].

For accelerating the abrasion process, the load is increased to 20 N. It can be seen that all coatings and even St3 steel suffer a greater loss of mass than in the case of 5 N shown in

graph 9. b. However, the mass loss of the laser coating was reduced in comparison with steel St3 and is asymptotically close to the plasma coating of CuSn, this is also consistent with studies of the hardness and structure of the inner layers of the alloy, where its hardness is higher and the structure has a higher homogeneity. The CuSn-Cr_xC_y plasma coating not only still exhibits superior abrasion resistance, but its track continues to bend than other coatings.

With the same samples, the load was increased to 50 N for testing, and the time between two measurements was 10 minutes. The results are shown in graph fig. 10. c. As shown in Table 1.2, plasma coatings are thick, about 1 mm, and laser coatings are low (200-300 μm). This is obvious at first, when the laser coating still had sublayers of alloys with high hardness and uniformity, but then the weight loss increased rapidly, which means that the abrasion process reached the base steel St3. Meanwhile, the plasma coatings continued to show good wear resistance, with the CuSn-CrxCy coating being the best.

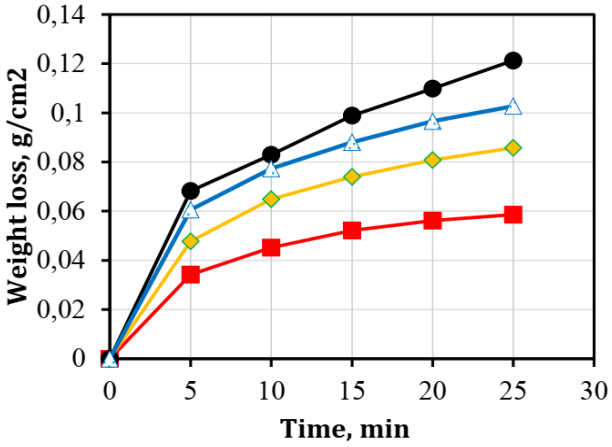

(a)

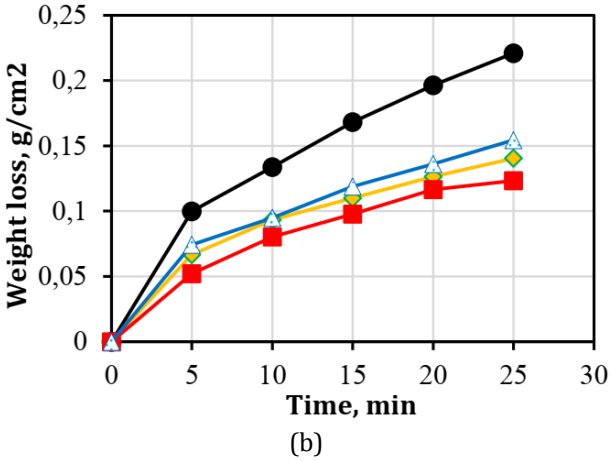

(b)

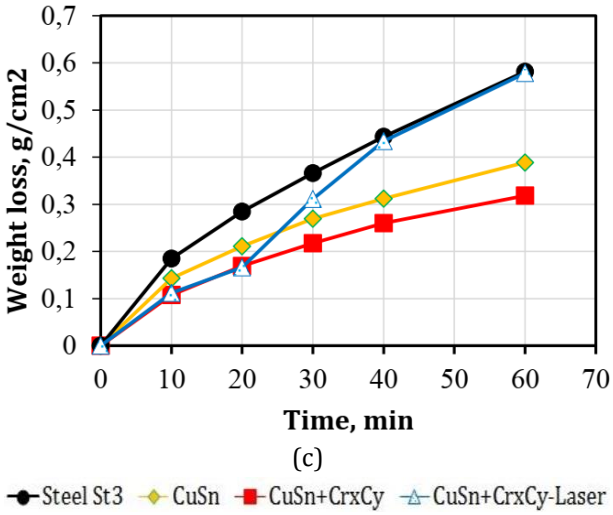

(c)

Steel St3 CuSn CuSn+CrxCy CuSn+CrxCy-Laser

Fig. 10. Weight loss of samples under loads: 5, 20, 50 N, (a) sandpaper – 220 SiC, load – 5 N, speed – 100 revs/min, water, (b) sandpaper – 220 SiC, load – 20 N, speed – 100 revs/min, water, (c) sandpaper – 220 SiC, load – 50 N, speed – 100 revs/min, water.

4. CONCLUSIONS

1. It has been established that there are differences in the geometry of the surface layer, structure and properties between plasma and laser heating of a mixture containing of the CuSn alloy and a coating of the welding electrode OK 84.78. During plasma treatment of the pre-coating, due to the larger heating spot, a much larger pool of molten metal and coating is formed, with a depth of fusion of the surface layer of about 1-2 mm and a width of 4-8 mm. After laser heating of the coating with overlapping reflow tracks (the track width is no more than 500 μm), the surface layer of the metal is melted to a maximum depth of 200 μm.
2. The addition of chromium carbide to the composition containing CuSn applied to the metal surface leads to an increase in the hardness of the surface layer after plasma treatment. Plasma coatings made from compositions containing 20% OK 84.78 have significantly high hardness, ranging from 460 to 700 HV.
3. The coatings formed after laser treatment (pulsed laser power supply) have many microcracks and low hardness in comparison with plasma coatings, which is in the range of 250-500 HV. Most of the hardness values of the laser coating are lower than those of the

plasma coating. This is because the exposure time during the laser coating surface melting is not enough to completely saturate the surface layer due to the small dissolution of bronze, chromium carbide and the main substrates into each other.

4. The coatings formed based on CuSn/CrxCy were superior in hardness to the CuSn coating, and the highest values were obtained because of plasma heating.
5. Measurement of abrasion showed that plasma coatings have higher wear resistance than laser coatings, whereby CuSn+CrxCy coatings have minimal weight loss. The wear resistance of all coatings is sufficiently higher than that of St3 steel, but the laser coating lost its mass faster with increasing load and test time.

REFERENCES

[1] Yu.M. Dombrovsky, *Physical foundations and technology of plasma surface hardening,* Hardening technologies and coatings, no. 3, pp. 14-25, 2007. (in Russian)

[2] A.E. Balanovskiy, *Main issues of plasma surface hardening of metals (Review. Part 1)*, Hardening technologies and coatings, no. 12, pp. 18-30, 2015. (in Russian)

[3] X. Cao, C. Li, L. Chen, B. Huang, *Experimental Study on the Design and Characteristics of a Laminar Plasma Torch With Medium Working Power and its Applications for Surface Hardening,* IEEE Transactions on Plasma Science, vol. 48, iss. 4, pp. 961-968, 2020, doi: 10.1109/TPS.2020.2979411

[4] X. Cao, D. Yu, M. Xiao, J. Miao, Y. Xiang, J. Yao, *Design and Characteristics of a Laminar Plasma Torch for Materials Processing*, Plasma Chem Plasma Process, vol. 36, pp. 693–710, 2016, doi: 10.1007/s11090-015-9661-6

[5] O.V. Chudina, V.A. Aleksandrov, S.I. Barabanov, A.A. Brezhnev, *Formation of a diffusion coating on the surface of steel by laser and thermal diffusion alloying*, Strengthening technologies and coatings, no. 4, pp. 37–40, 2010. (in Russian)

[6] O.V. Chudina, A.A. Brezhnev, *Surface alloying of carbon tool steels using laser heating*, Strengthening technologies and coatings, vol. 2015, iss. 13, pp. 1090-193, 2010, doi: 10.1134/S0036029515130030

[7] A.E. Balanovskiy, V.V. Huy, *Saturation of the metal surface with carbon during plasma surface treatment*, Strengthening technologies and coatings, vol. 13, no. 9, pp. 403-415, 2017 (in Russian).

[8] B.S. Ünlü, E. Atik, *Evaluation of effect of alloy elements in copper based CuSn10 and CuZn30 bearings on tribological and mechanical properties*, Journal of Alloys and Compounds, vol. 489, iss. 1, pp. 262-268, 2010, doi: 10.1016/j.jallcom.2009.09.068

[9] I. Mabille, A. Bertrand, E.M.M. Sutter, C. Fiaud, *Mechanism of dissolution of a Cu–13Sn alloying low aggressive conditions*, Corrosion Science, vol. 45, iss. 5, pp. 855-866, 2003, doi: 10.1016/S0010-938X(02)00207-X

[10] X. Guo, G. Zhang, W. Li, Y. Gao, H. Liao, C. Coddet, *Investigation of the microstructure and tribological behavior of cold-sprayed tin-bronze-based composite coatings*, Applied Surface Science, vol. 255, iss. 6, pp. 3822-3828, 2009, doi: 10.1016/j.apsusc.2008.10.041

[11] K.S Tan, R.J.K Wood, K.R Stokes, *The slurry erosion behaviour of high velocity oxy-fuel (HVOF) sprayed aluminium bronze coatings*, Wear, vol. 255, iss. 1-6, pp. 195-205, 2003, doi: 10.1016/S0043-1648(03)00088-7

[12] X. Dai, S. Zhou, M. Wang, J. Lei, C. Wang, T. Wang, *Microstructure evolution of phase separated Fe-Cu-Cr-C composite coatings by laser induction hybrid cladding*, Surface and Coatings Technology, vol. 324, pp. 518-525, 2017, doi: 10.1016/j.surfcoat.2017.06.032

[13] F. Arias-González, J. del Val, R. Comesañ, J. Penide, F. Lusquiños, F. Quintero, A. Riveiro, *Production of phosphor bronze coatings by laser cladding*, Procedia Manufacturing, vol. 13, pp. 177-182, 2017, doi: 10.1016/j.promfg.2017.09.031

[14] Q.Y. Hou, T.T. Ding, Z.Y. Huang, P. Wang, L.M. Luo, Y.C. Wu*Microstructure and properties of mixed Cu–Sn and Fe-based alloys without or with molybdenum addition processed by plasma transferred arc*, Surface and Coatings Technology, vol. 283, pp.184-193, 2015, doi: 10.1016/j.surfcoat.2015.10.043

[15] K.S. Al-Athel, M. Ibrahim, Arif, *Effect of Composition and Thickness on the Hardness and Scratch Resistance of Copper and Copper Alloy Coatings*, Arabian Journal for Science and Engineering, vol. 42, pp. 4895–4904, 2017, doi: 10.1007/s13369-017-2661-5

[16] X. Yin, F. Xu, C. Min, Y. Cheng, X. Dong, B. Cui, D. Xu, *Promoting the bonding strength and abrasion resistance of brazed diamond using Cu–Sn–Ti composite alloys reinforced with tungsten carbide*, Diamond and Related Materials, vol. 112, Available online, 2021, doi: 10.1016/j.diamond.2021.108239

[17] A.E. Balanovsky, V.V. Huy, *Estimation of Wear Resistance of Plasma-Carburized Steel Surface in Conditions of Abrasive Wear*, vol. 39, iss. 4, pp. 311-318, 2018, doi: 10.3103/S1068366618040025

[18] GOST 3647-80, *Abrasives. Grain sizing. Graininess and fraction. Test methods.* 1980. (in Russian)